Study of nonminimum phase zeros in test power systems from wide-area control designs

Mohammadreza Hatami, Vaithianathan "Mani" Venkatasubramanian, and Sandip Roy,
School of EECS, Washington State University, Pullman, WA
Email: mani@eecs.wsu.edu

Patrick Panciatici, Florent Xavier, and Thibault Prevost
RTE France, Paris, France

***Abstract*— This paper is aimed at studying the presence of non-minimum phase zeros which can emerge in the design of modern wide-area controls in the power network. Zeros in the open right half complex plane can make the design of controllers challenging. The study includes two wide-area control designs on the well-known two-area Kundur system. In the first case, power system stabilizers (PSSs) are designed using both local and remote signals. In the second case, the presence of non-minimum phase zeros in damping controller design for static var compensators (SVCs) is examined. The case studies highlight the prevalence of right half plane zeros and zeros at infinity in wide-area control designs which points to the complexity of this emerging problem in synchrophasor based designs of the future. Some of the computational issues need attention as well. For instance, it is pointed out that the numerical accuracy of the linearized model can influence the calculation of very small zeros, moving them from left to right half complex plane and vice versa.**

***Index Terms*— wide-area control designs, synchrophasors, generalized eigenanalysis, non-minimum phase dynamics, power system input-output characteristics, transfer function zeros.**

I. INTRODUCTION

Recent advances in wide-area monitoring technology using synchrophasors have led to renewed interest in the design of wide-area controls for the bulk power transmission network, to shape small-signal and transient characteristics of the swing dynamics. Evaluation and design of such wide-area controls require analysis of the input-to-output characteristics of control channels. In particular, control designs for small-signal stability enhancement are often based on pole-zero characteristics of a linearized input-output model, see e.g. [1]. The poles (modes) of the swing dynamics, which are internal properties of the network (unrelated to the specific control channel considered), have been extensively characterized [2]-[3]. In contrast, there has been relatively little work on the zeros of the swing dynamics models.

The zeros of a linear model, or more explicitly its finite- and infinite- zero structure, are invariants to feedback and hence play a crucial role in analysis and design of controls. In particular, the zeros guide the structure of control designs, and place essential limits on control performance as well as the effort required for control. The reader is referred to the articles [4]-[5] for an overview of computation of linear system zeros, and the importance of zeros to control analysis and design. Precisely, the infinite-zero structure of the network decides the required dynamic complexity of the controller. Meanwhile, the presence of finite zeros in the right half plane (RHP), also known as non-minimum phase zeros, places essential limits on control performance and effort. For instance, as mentioned in [6], RHP zeros limit the maximum achievable bandwidth of HVDC controllers.

Other characteristics of the finite zeros, such as near pole-zero cancellations and poorly-damped left-half-plane (LHP) zeros, also influence control design and performance. Given this tight link between the zeros and control design, there is significant motivation to characterize the finite- and infinite-zero structure of linearized swing-dynamics models.

A few previous works have considered the computation and analysis of the zeros of the power system swing dynamics. The pioneering work by Martins et al. in [7] proposed methods for studying transfer function zeros in large-scale power system models. Authors of [8] have suggested creating an inverse system for the original system, whose poles are the zeros of the original system. Moreover, two methods for calculating a few dominant zeros which are close to a pre-specified point in the s-plane is suggested in the paper [8].

Same as the system poles, the system zeros change by changing the system operating point, since the system is non-linear. As reported in [9], a pair of complex conjugate RHP zeros can appear suddenly in real-time implementations, even though it may be absent in a set of input-output data at the present time. Moreover, the occasional presence of a zero close to a system mode can cause intermittent oscillation of the mode [9]. In summary, since the closed loop performance of the controllers highly depends on the presence of RHP zeros, the zeros should be monitored along with the estimation of system modes.

Authors of [10]-[11] have proposed four indicators for selecting the most appropriate remote feedback signals for designing auxiliary inter-area damping controllers on FACTS devices. It is mentioned that outputs which produce non-minimum phase zeros are undesirable, since by increasing the feedback gain, they may lead to gain instability. Therefore, as

one indicator, remote output signals with RHP zeros in the range of 0.1Hz to 2Hz are discarded from the candidate signals, even if they have higher controllability and observability indices comparing to the minimum-phase channels.

Analytical conditions were proposed in [12] for when RHP zeros can appear in general power system dynamics represented by classical angle stability models using swing equations. The work is extended in [13] where the effect of one control channel (especially HVDC line) on the finite zeros of the other input-output channels is characterized.

In this paper, we study the finite- and infinite- zero structures of detailed models of test power systems, focusing especially on the presence and impact of RHP transfer function zeros. Linearization of detailed swing-dynamics models are first undertaken using the commercial program Small-Signal Analysis Tool (SSAT) [14] Then zeros are characterized for control channels of interest, for both the cases where the input and output are collocated (at the same bus) and where they are from different buses. Simulations include the study of zeros in two cases; PSS design and SVC damping controller design. The exciter control voltage reference and the SVC voltage control reference are the input locations, respectively. The outputs of interest are generator speed deviations, bus voltage magnitudes, bus voltage angles, bus angle differences, line current magnitudes, and line active power-flows. The studies show that in the case of traditional PSS design with local feedback, there is no RHP zero in the transfer function; however, the choice of remote output signals leads to non-minimum phase dynamics for most signals. Some numerical issues related to the zero computation are also highlighted. For example, it is shown that RHP zeros can be incorrectly calculated as LHP zeros or vice versa by using inaccurate power-flow solutions.

The rest of the paper is organized as follows. Section II describes the modeling and the algorithm used for calculating power system transfer function zeros. Case studies as well as observations are discussed in Section III. Section IV contains a brief conclusion and suggested future work.

II. CALCULATION OF TRANSFER FUNCTION ZEROS

A. Power system small signal modeling

Power system dynamics can be represented by Differential-Algebraic Equations (DAE) as follows.

$$\begin{aligned} \dot{x} &= f(x, y) \\ 0 &= g(x, y) \end{aligned} \tag{1}$$

Here x and y are n- and 2m-dimensional vectors denoting the dynamic states and the network states, respectively.

For small signal analysis, the above non-linear equations can be linearized around an equilibrium point. Due to special structure of power systems, one may separately linearize the equations of each dynamic device and then aggregate all of them to obtain the overall system linearized DAE equations [15]. Each individual device can be modeled by the set of equations (2).

$$\begin{cases} \dot{x}_i = A_{d_i} x_i + B_{d_i} \Delta v \\ \Delta i_i = C_{d_i} x_i - D_{d_i} \Delta v \end{cases} \tag{2}$$

in which x_i is the state vector of the i^{th} device, i_i is the injected current into the network from the device, v is the vector of the network bus voltages.

The network states y in (2). contain the bus voltage information. They can be presented either in polar form (i.e., the bus voltage magnitudes and bus voltage angles) or in Cartesian form (i.e., voltage phasor real and imaginary parts). In this work, the latter Cartesian form which is employed in DSATools [14] is used.

Aggregating all equations of individual devices to obtain the overall system equations results in (3).

$$\begin{cases} \dot{x} = A_D x + B_D \Delta v \\ \Delta i = C_D x + D_D \Delta v \end{cases} \tag{3}$$

Here x is the state vector of the overall system which is made by stacking up all the x_i device state vectors together. $A_D, B_D, C_D,$ and D_D are block diagonal matrices built by assembling $A_i, B_i, C_i,$ and D_i associated with the individual devices.

The transmission system connects the dynamic devices together and is modeled by the algebraic equations in the form of (4).

$$\Delta i = Y_N \Delta v \tag{4}$$

In above equations, $A_D, B_D, C_D, D_D,$ and Y_N matrices are all real-valued and have dimensions $n \times n$, $n \times 2m$, $2m \times n$, $2m \times 2m$, and $2m \times 2m$, respectively, where n and m are the total number of states and number of system buses.

The overall state matrix of the system can be calculated by substituting (4) into (3) as follows [15].

$$A = A_D + B_D (Y_N - D_D)^{-1} C_D \tag{5}$$

This equation will be later used for simplifying the computation of transfer function zeros.

B. Transfer function zeros calculation

Let us consider the state equations of a general DAE system, i.e. a control channel or input-to-output map, as given in (6). A single-input single-output study of power system is of interest of this study.

$$\begin{aligned} E\dot{x}(t) &= A_c x(t) + B_c u(t) \\ y(t) &= C_c x(t) + D_c u(t) \end{aligned} \tag{6}$$

In order to distinguish matrices with the same symbol, the index (subscript) *C* is used for control-channel (input-to-output system) matrices (i.e., input, output, and feedthrough matrices) and the index *D* for matrices derived from linearizing the DAE equations.

The zeros of the DAE system are defined as λ values in (7) such that the rank of the following matrix drops below its normal rank [16].

$$\begin{bmatrix} A_c - \lambda E & B_c \\ C_c & D_c \end{bmatrix} \tag{7}$$

In the power systems model, the descriptor matrix E is the identity matrix of dimension of the system state matrix. Thus, for the rest of this work, the general descriptor matrix E will be substituted by the identity matrix I.

By substituting A_C from (5) into (7), we get that the zeros are λ values such that the following matrix (8) loses rank:

$$\begin{bmatrix} A_D + B_D(Y_N - D_D)^{-1}C_D - \lambda I & B_c \\ C_c & D_c \end{bmatrix} \tag{8}$$

From a computational point of view, it would be preferable to avoid taking the inverse $(Y_N - D_D)$, since inverting such a large matrix is time consuming.

Based on the definition in (7), system zeros make the determinant of (8) equal to zero. Considering $\det(\begin{bmatrix} A_1 & A_2 \\ A_3 & A_4 \end{bmatrix}) = \det(A_4)\det(A_1 - A_2 A_4^{-1} A_3)$, the determinant of (8) can be written as (9):

$$\begin{aligned} \det(D_c)\det((A_D + B_D(Y_N - D_D)^{-1}C_D - \lambda E) \\ - B_c D_c^{-1} C_c) = 0 \end{aligned} \tag{9}$$

Provided that $\det(D_c) \neq 0$, we have:

$$\det((A_D + B_D(Y_N - D_D)^{-1}C_D - \lambda E) - B_c D_c^{-1} C_c) = 0 \tag{10}$$

Multiplying both sides of (10) by $\det(Y_N - D_D)$ and rearranging results in (11).

$$\begin{aligned} \det(Y_N - D_D)\det(\underbrace{(A_D - B_c D_c^{-1} C_c - \lambda E)}_{n*n\ matrix} - \\ (\underbrace{-B_D}_{n*2m\ \text{matrix}})\underbrace{(Y_N - D_D)^{-1}}_{2m*2m\ \text{matrix}}\underbrace{C_D}_{2m*n\ \text{matrix}}) = 0 \end{aligned} \tag{11}$$

The left side of (11) is the determinant of the matrix represented in (12).

$$\begin{bmatrix} A_D - B_c D_c^{-1} C_c - \lambda E & -B_D \\ C_D & Y_N - D_D \end{bmatrix} \tag{12}$$

Finding transfer function zeros using (12) instead of (8) has the advantage of not requiring inversion of the matrix $(Y_N - D_D)$. For SISO systems, the *D* matrix is $1*1$, and hence easy to invert. However, for most power systems' input-output pairs, the feedthrough matrix is zero. Thus, (8) needs to be refined to a more general form. This can be done as follows.

For each λ value in (8), the vector $v = \begin{bmatrix} w_1 & w_2 \end{bmatrix}^T$ can be found such that (13) holds.

$$\begin{bmatrix} A_D + B_D(Y_N - D_D)^{-1}C_D - \lambda E & B_C \\ C_C & D_C \end{bmatrix}\begin{bmatrix} w_1 \\ w_2 \end{bmatrix} = \underline{0} \tag{13}$$

To eliminate $(Y_N - D_D)^{-1}$ in the expression, the vector w_3 can be defined as (14).

$$(Y_N - D_D)^{-1} C_D w_1 = w_3 \tag{14}$$

By substituting $B_D(Y_N - D_D)^{-1}C_D w_1$ with $B_D w_3$ and including $C_D w_1 - w_3(Y_N - D_D) = 0$ into the sets of equations, the more efficient form (15) can be obtained.

$$\begin{bmatrix} A_D - \lambda E & B_C & B_D \\ C_C & D_C & 0 \\ C_D & 0 & -(Y_N - D_D) \end{bmatrix}\begin{bmatrix} w_1 \\ w_2 \\ w_3 \end{bmatrix} = \underline{0} \tag{15}$$

Equation (15) is a generalized eigenvalue problem. For large-scale power systems, when only a few of zeros are of interest, the problem can be solved by means of efficient algorithms. We notice that the zeros analysis described here closely follows the development in [8].

By using (15) instead of (7), the number of calculated zeros increases by $2m$. The spurious additional zeros are found at infinity, i.e. the set of finite zeros remains the same.

III. CASE STUDIES

The two-area test system described in [15] which is well known for displaying inter-area oscillations is considered for this study. The single line diagram of this system is depicted in Figure 1. Under high power transfers, it can be shown that the system has a poorly damped inter-area mode [15]. Traditional power system stabilizer (PSS) designs using local generator signals are discussed in detail in [17]-[19] for improving the damping of this inter-area mode.

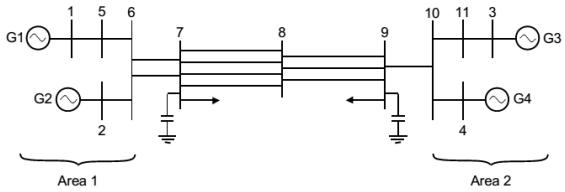

Figure 1. Two-area Kundur test system [15]

The study includes two parts. In the first part, the zeros for traditional PSS design as well as a design based on remote signals such as line current magnitude and active power are studied. The second part studies the presence of RHP zeros for SVC auxiliary damping control design for both local and remote channels.

A. PSS design

We are interested in the design of PSSs using both local and remote output signals. Suppose we consider the PSS design for Generator 1, then, the exciter control voltage reference V_{ref_1} is set to be the input. It is worth mentioning that the PSS of the generator at input location is disabled, whereas other generators are equipped with PSSs. The output is assumed to be taken from six choices of signals; generator speed deviation, bus voltage magnitude, bus voltage angle, bus angle difference, line current magnitude, and line active power

1) Generator speed signals

Table 1 shows the transfer function finite zeros when V_{ref_1} is the input and generator speed signals are outputs. . In addition, the transfer function is found to have three infinite zeros (relative degree 3) for each output. The RHP zeros are bold in the table. Only for this case, all the finite zeros are shown. For other cases, for the sake of brevity, only RHP zeros and LHP zeros whose real value is greater than -10 are shown. It is interesting that there is no RHP zero for the traditional PSS design (i.e., while using generator 1 speed as the output). The same result is analytically shown in [12] where all the zeros of a local transfer function are in LHP for the classical generator model.

TABLE I. SYSTEM ZEROS WHEN OUTPUTS ARE GENERATOR SPEED SIGNALS

Output signal			
ω_1	ω_2	ω_3	ω_4
0.0000+0.0000i	0.0000+0.0000i	0.0000+0.0000i	0.0000+0.0000i
-0.5070+0.0000i	-0.4956+0.0000i	-0.5000+0.0000i	-0.5000+0.0000i
-0.5096+0.0000i	-0.5000+0.0000i	-0.5101+0.0000i	-0.5089+0.0000i
-0.5695+0.0000i	-0.5094+0.0000i	-0.5155+0.0000i	-0.5155+0.0000i
-0.7955+1.4030i	-1.3007+0.0000i	-1.6967+0.0000i	-1.6832+0.0000i
-0.7955-1.4030i	-2.3812+0.0000i	-2.5944+0.0878i	-2.2203+0.0000i
-2.3980+0.0000i	-3.3562+0.0000i	-2.5944-0.0878i	-3.0159+0.0000i
-3.1848+0.0000i	-3.4950+0.0000i	-3.4056+0.0000i	-3.4103+0.0000i
-4.3250+0.0698i	**0.1449+3.9114i**	-6.1043+0.0000i	-6.3516+0.0000i
-4.3250-0.0698i	**0.1449-3.9114i**	-0.8262+7.9503i	-0.6508+6.6966i
-0.6170+5.0710i	**3.9574+0.0000i**	-0.8262-7.9503i	-0.6508-6.6966i
-0.6170-5.0710i	-7.0017+0.0000i	-8.5763+0.3809i	**7.0961+0.0000i**
-0.7872+7.4944i	-0.7869+7.4923i	-8.5763-0.3809i	-0.9231+8.0755i
-0.7872-7.4944i	-0.7869-7.4923i	-1.0543+8.6834i	-0.9231-8.0755i
-8.7575+0.0000i	-8.7201+0.0000i	-1.0543-8.6834i	-8.2046+0.0000i
-10.301+0.0000i	-15.5660+7.3467i	**9.1771+0.0000i**	-10.7185+0.0000i
-14.378+8.8779i	-15.5660-7.3467i	-22.878+3.9125i	-21.429+4.4108i
-14.3786-8.8779i	-20.4752+0.0000i	-22.8787-3.9125i	-21.4296-4.4108i
-20.8717+0.0000i	-13.5504+17.4012i	-23.1703+4.7750i	-22.9932+4.2642i
-20.5606+4.2459i	-13.5504-17.4012i	-23.1703-4.7750i	-22.9932-4.2642i
-20.5606-4.2459i	-22.4630+4.4329i	-25.0000+0.0000i	-25.0000+0.0000i
-22.4635+4.4318i	-22.4630-4.4329i	-25.0000+0.0000i	-25.0000+0.0000i
-22.4635-4.4318i	-25.0000+0.0000i	-28.7828+0.0000i	-9.0491+23.3955i
-28.7530+0.0000i	-25.0000+0.0000i	-1.6847+28.8457i	-9.0491-23.3955i
-29.3360+0.0000i	-28.7519+0.0000i	-1.6847-28.8457i	-28.7658+0.0000i
-31.5719+0.0000i	-30.8339+0.0000i	-30.2531+0.0000i	-30.4904+0.0000i
-32.7039+0.0000i	-32.9218+0.2756i	-32.4729+0.0000i	-32.8641+0.0000i
-33.3012+0.0000i	-32.9218-0.2756i	-33.5373+0.0000i	-33.8350+0.0000i
-35.4668+0.0000i	-34.5527+0.0000i	-38.7999+0.2745i	-35.8535+0.0000i
-37.2776+0.0000i	-37.2689+0.0000i	-38.7999-0.2745i	-38.7657+0.0000i
-51.8299+0.0000i	-51.8306+0.0000i	-51.4542+0.2405i	-51.3925+0.0000i
-52.3609+0.0000i	-52.7310+0.0000i	-51.4542-0.2405i	-52.1878+0.0000i
-52.8413+0.0000i	-53.5758+0.0000i	-54.2328+0.0000i	-53.9522+0.0000i
-66.6666+0.0000i	-66.6667+0.0000i	-66.6667+0.0000i	-66.6667+0.0000i

If any other generator speed is used as the output for the transfer function (which would then be the input for the generator 1 PSS design), the transfer function has RHP zeros some real and some complex conjugate. It is interesting that this is different from the results in [12], where there is no RHP zero if there is only one path between the input and the output nodes.

It is noted that similar results are obtained when other generators are examined; showing no RHP zero for local output and having real and complex conjugate zeros for remote speed signals.

It should be mentioned that for all generator speed signals, one zero at origin is found. This is because of the fact that the generator speed signal is basically the time-derivative of the respective generator rotor angle. This corresponds to an *s* in Laplace domain (i.e., a zero at origin).

The *authors thank RTE France, Power System Engineering Research Center (PSERC), US Department of Energy and US National Science Foundation for supporting this work.*

2) Bus voltage magnitude signals

Table II shows the zeros of the input V_{ref_1} paired with bus voltage magnitudes as outputs. In this case, the transfer function has exactly two RHP zeros for each choice of voltage magnitude signals V_1 through V_{11}.

TABLE II. SYSTEM ZEROS WHEN OUTPUTS ARE BUS VOLTAGE MAGNITUDE SIGNALS

Output signal			
V_1	V_2	V_3	V_4
0.0002+0.0083i	**0.0120+0.0000i**	**0.0130+0.0000i**	**0.0128+0.0000i**
0.0002-0.0083i	**0.2649+0.0000i**	-2.1034+0.3804i	**1.9520+0.0000i**
-3.4633+0.2021i	-3.4095+0.0958i	-2.1034-0.3804i	-0.2845+5.0235i
-3.4633-0.2021i	-3.4095-0.0958i	**2.8555+0.0000i**	-0.2845-5.0235i
-0.1359+4.4406i	-0.1567+4.7821i	-0.2699+5.1795i	-0.8143+7.7220i
-0.1359-4.4406i	-0.1567-4.7821i	-0.2699-5.1795i	-0.8143-7.7220i
-0.9314+7.3892i	-0.8063+7.4952i	-0.8851+7.7263i	-0.4255+7.9074i
-0.9314-7.3892i	-0.8063-7.4952i	-0.8851-7.7263i	-0.4255-7.9074i
-0.7833+7.5091i	-0.3336+7.8854i	-8.0251+0.4586i	-
-0.7833-7.5091i	-0.3336-7.8854i	-8.0251-0.4586i	-
-	-	-0.4176+8.0459i	-
-	-	-0.4176-8.0459i	-

V_5	V_6	V_7	V_8
0.0002+0.0088i	**0.0002+0.0105i**	**0.0002+0.0096i**	**0.0001+0.0107i**
0.0002-0.0088i	**0.0002-0.0105i**	**0.0002-0.0096i**	**0.0001-0.0107i**
-3.4302+0.1647i	-3.4043+0.1118i	-3.3965+0.1089i	-3.3686+0.1019i
-3.4302-0.1647i	-3.4043-0.1118i	-3.3965-0.1089i	-3.3686-0.1019i
-0.1556+4.5615i	-0.1498+4.8921i	-0.1285+5.0348i	-0.0712+5.3521i
-0.1556-4.5615i	-0.1498-4.8921i	-0.1285-5.0348i	-0.0712-5.3521i
-0.8125+7.5039i	-0.8087+7.5046i	-0.8149+7.5120i	-0.8370+7.5371i
-0.8125-7.5039i	-0.8087-7.5046i	-0.8149-7.5120i	-0.8370-7.5371i
-0.8036+7.6524i	-0.5157+7.9446i	-0.4973+7.9255i	-0.4463+7.8745i
-0.8036-7.6524i	-0.5157-7.9446i	-0.4973-7.9255i	-0.4463-7.8745i

V_9	V_{10}	V_{11}
0.0084+0.0485i	**0.0223+0.0000i**	**0.0513+0.0000i**
0.0084-0.0485i	**0.6170+0.0000i**	**1.7543+0.0000i**
-0.1797+5.0358i	-0.4656+4.7449i	-2.2109+0.2490i
-0.1797-5.0358i	-0.4656-4.7449i	-2.2109-0.2490i
-0.8678+7.6559i	-0.8519+7.6841i	-0.7248+4.8127i
-0.8678-7.6559i	-0.8519-7.6841i	-0.7248-4.8127i
-0.4095+7.9179i	-0.4239+7.9716i	-0.8621+7.7287i
-0.4095-7.9179i	-0.4239-7.9716i	-0.8621-7.7287i
-	-	-0.3925+8.0357i
-	-	-0.3925-8.0357i
-	-	-8.3553+0.3835i
-	-	-8.3553-0.3835i

As can be seen from Table IV, for some outputs such as V_1, there is a pair of conjugate zeros which are very small in magnitude. Now, naturally, a question arises as to whether these zeros are caused by numerical issues or they are genuine. Because of not using the relative rotor angles in small signal modeling, an eigenvalue at origin is expected. Depending on the power flow solution mismatch, this eigenvalue will be calculated somewhere around the origin. For instance, in the two-area system used in this study, this eigenvalue is calculated as $\lambda = +0.082$ and $\lambda = -0.000031 \pm 0.00902\text{i}$ when power flow mismatch is chosen as 1MW and 0.001MW, respectively.

This suggests that the zeros close to origin might be inaccurate. The root locus analysis proposes that by increasing the feedback gain, the poles of the closed-loop system approaches to the system zeros. Thus, in order for validating the zeros calculation, one may perform the root locus analysis either by manipulating the effect of feedback in the system state matrix or by adding the appropriate feedback into the model. Although investigation on this example shows that the poles of closed-loop system approaches to the (very small) zeros, this is not a valid approach, since both of the open-loop and closed-loop systems are derived with the same level of power flow accuracy.

A closer scrutiny reveals that the accuracy of power flow solution highly effects the zeros calculation, especially those which are close to the origin. Table III shows the calculated zeros for some cases with trivial zeros. Two values for power flow mismatch are considered.

Table III. EFFECT OF POWER FLOW ACCURACY ON CALCULATED ZEROS

Power flow mismatch (MW)	Output signals			
	V_1	V_2	V_3	$\delta_1 - \delta_5$
1 (default value)	0.0830	0.3173	$-0.0086 \pm 0.0942\text{i}$	0.0758 -0.0708
0.001	$0.0002 \pm 0.0083i$	0.0120	0.0130	$-0.0002 \pm 0.0294i$

It can be observed from Table III that by increasing the power flow solution accuracy, some RHP zeros move into LHP, and vice versa. Moreover, some real-valued zeros have disappeared and two new oscillatory zeros emerge, and vice versa. Since the power mismatch 0.001MW is the smallest value feasible in the software used, further investigation on the role of power flow solution accuracy is left as an open question.

3) Bus voltage angle signals

Table IV shows the system zeros when bus voltage angles are set as outputs (even for the local bus voltage δ_1). . It can be seen that a real-valued RHP zero is present when the output is any of the bus voltage angles. For some buses, complex conjugate zeros are observed as well.

4) Bus voltage angle difference signals

The system zeros when the input V_{ref_1} is paired with some bus voltage angle differences is shown in Table V. The choices include connected buses such as Buses 1 and 5, and also buses which are across the system such as Buses 6 and 10. Same as for the choice of bus voltage phase angles, real-valued RHP zeros can be observed for all choices.

It is notable that similar to the case where bus voltage magnitude signals were chosen as output, very small zeros are observed in this case.

Table IV. SYSTEM ZEROS WHEN OUTPUTS ARE BUS VOLTAGE ANGLE SIGNALS

Output signal			
δ_1	δ_2	δ_3	δ_4
-0.6113+3.0970i	-0.3153+3.5868i	-0.9696+7.8666i	-0.4158+6.9725i
-0.6113-3.0970i	-0.3153-3.5868i	-0.9696-7.8666i	-0.4158-6.9725i
5.5692+0.0000i	**7.1682+0.0000i**	-0.6218+8.1561i	-0.8402+7.9783i
-1.0439+6.1866i	-0.7892+7.4895i	-0.6218-8.1561i	-0.8402-7.9783i
-1.0439-6.1866i	-0.7892-7.4895i	-8.5869+2.3532i	-9.5782+2.0608i
-0.7868+7.4974i	**0.2248+10.0517i**	-8.5869-2.3532i	-9.5782-2.0608i
-0.7868-7.4974i	**0.2248-10.0517i**	**5.3558+8.1234i**	**3.1768+9.6458i**
-	-	**5.3558-8.1234i**	**3.1768-9.6458i**
-	-	**19.7192+0.0000i**	**11.3941+0.0000i**

δ_5	δ_6	δ_7	δ_8
-0.5241+3.3261i	-0.3840+3.6335i	-0.3812+3.7340i	-0.3661+4.0696i
-0.5241-3.3261i	-0.3840-3.6335i	-0.3812-3.7340i	-0.3661-4.0696i
5.5325+0.0000i	**5.9555+0.0000i**	**5.9278+0.0000i**	**5.9447+0.0000i**
-1.1214+6.7158i	-0.7962+7.4878i	-0.7974+7.4902i	-0.8023+7.5003i
-1.1214-6.7158i	-0.7962-7.4878i	-0.7974-7.4902i	-0.8023-7.5003i
-0.7866+7.5005i	-0.8373+8.2490i	-0.8313+8.2495i	-0.8146+8.2563i
-0.7866-7.5005i	-0.8373-8.2490i	-0.8313-8.2495i	-0.8146-8.2563i

δ_9	δ_{10}	δ_{11}
0.0270+6.2705i	-0.0804+7.0988i	-0.9341+7.7698i
0.0270-6.2705i	-0.0804-7.0988i	-0.9341-7.7698i
7.5913+0.0000i	-0.7919+7.8317i	-0.5208+8.0270i
-0.8120+7.6956i	-0.7919-7.8317i	-0.5208-8.0270i
-0.8120-7.6956i	**0.4936+8.6195i**	-8.9372+2.6837i
-0.4680+8.4895i	**0.4936-8.6195i**	-8.9372-2.6837i
-0.4680-8.4895i	**8.8036+0.0000i**	**2.9845+8.8676i**
-	-	**2.9845-8.8676i**
-	-	**11.6352+0.0000i**

Table V. SYSTEM ZEROS WHEN OUTPUTS ARE BUS VOLTAGE ANGLE DIFFERENCE SIGNALS

Output signal			
$\delta_1-\delta_5$	$\delta_5-\delta_6$	$\delta_6-\delta_7$	$\delta_7-\delta_8$
-0.0002+0.0294i	**0.0414+0.0000i**	-0.0021+0.0721i	**0.0480+0.0000i**
-0.0002-0.0294i	**4.2376+0.0000i**	-0.0021-0.0721i	**5.7816+0.0000i**
-0.3191+4.9056i	-0.3763+4.9756i	**6.8704+0.0000i**	-0.7719+7.4487i
-0.3191-4.9056i	-0.3763-4.9756i	-0.7722+7.4491i	-0.7719-7.4487i
5.8482+0.0000i	-0.7880+7.4944i	-0.7722-7.4491i	-0.8952+8.2094i
-0.7878+7.4942i	-0.7880-7.4944i	-0.9378+8.2228i	-0.8952-8.2094i
-0.7878-7.4942i	-	-0.9378-8.2228i	-

$\delta_8-\delta_9$	$\delta_9-\delta_{10}$	$\delta_{10}-\delta_{11}$	$\delta_4-\delta_{10}$
-0.0003+0.0357i	-0.0008+0.0481i	**0.0671+0.0000i**	**0.0708+0.0000i**
-0.0003-0.0357i	-0.0008-0.0481i	**5.1461+0.0000i**	**4.6575+0.0000i**
4.3942+0.0000i	**4.0368+0.0000i**	-0.8440+7.9072i	-0.7786+6.7901i
-0.7714+7.4483i	-0.7713+7.4481i	-0.8440-7.9072i	-0.7786-6.7901i
-0.7714-7.4483i	-0.7713-7.4481i	-8.6054+0.5018i	-0.8937+8.1125i
-0.8394+8.1864i	-0.8256+8.1796i	-8.6054-0.5018i	-0.8937-8.1125i
-0.8394-8.1864i	-0.8256-8.1796i	-0.5664+8.6617i	-
-8.7935+0.1514i	-	-0.5664-8.6617i	-
-8.7935-0.1514i	-	-	-

5) Line currents signals

Table VI shows the system zeros when the magnitude of line current signals are of interest. For each choice of line, at least there is one RHP zero. Moreover, all RHP zeros are real-valued.

6) Line active power signals

The line active power signal is another good candidate to examine, since inter-area oscillations are clearly seen in line flows. Table VII shows transfer function zeros when line active power signals are of interest. Similar to line current and bus angle difference cases, at least one RHP zero is observed for each choice.

Table VI. SYSTEM ZEROS WHEN OUTPUTS ARE LINE CURRENTS SIGNALS

Output signal			
I_{1-5}	I_{5-6}	I_{6-7}	I_{7-8}
-0.0024+0.0634i	**0.0833+0.0000i**	-0.0230+0.1509i	**0.0553+0.0000i**
-0.0024-0.0634i	-1.1529+0.1324i	-0.0230-0.1509i	**3.9888+0.0000i**
-1.1626+0.0749i	-1.1529-0.1324i	**1.0954+0.0000i**	-0.7754+7.4566i
-1.1626-0.0749i	**1.4836+0.0000i**	-1.3865+0.9526i	-0.7754-7.4566i
1.5280+0.0000i	-0.4991+5.0492i	-1.3865-0.9526i	-0.8167+8.1857i
-0.4973+5.0475i	-0.4991-5.0492i	-2.1861+0.2355i	-0.8167-8.1857i
-0.4973-5.0475i	-0.7876+7.4945i	-2.1861-0.2355i	-8.6656+0.3392i
-0.7876+7.4945i	-0.7876-7.4945i	-3.3390+0.3354i	-8.6656-0.3392i
-0.7876-7.4945i	-	-3.3390-0.3354i	-
-	-	-0.7826+7.4708i	-
-	-	-0.7826-7.4708i	-
-	-	-0.7129+8.1309i	-
-	-	-0.7129-8.1309i	-

I_{8-9}	I_{9-10}	I_{10-11}	I_{4-10}
-0.0004+0.0381i	-0.0005+0.0515i	**0.0701+0.0000i**	**0.0853+0.0000i**
-0.0004-0.0381i	-0.0005-0.0515i	**5.9969+0.0000i**	**4.7032+0.0000i**
3.5574+0.0000i	**5.3437+0.0000i**	-0.8411+7.9246i	-0.7259+6.7899i
-0.7752+7.4560i	-0.7531+7.4160i	-0.8411-7.9246i	-0.7259-6.7899i
-0.7752-7.4560i	-0.7531-7.4160i	-8.5000+0.4944i	-0.8968+8.0969i
-0.8006+8.1760i	-0.8921+8.1627i	-8.5000-0.4944i	-0.8968-8.0969i
-0.8006-8.1760i	-0.8921-8.1627i	-0.7306+8.7083i	-
-8.5502+0.1820i	-	-0.7306-8.7083i	-
-8.5502-0.1820i	-	-	-

7) Summary

Traditional PSS design uses local machine speed signal or local machine accelerating power signal as feedback input signals. However, if non-traditional signals such as active power-flow on tie-lines are used, Tables I to VII show that the use of non-traditional signals can introduce right half plane zeros in almost all the cases. Potential numerical issues in the case of analyzing remote bus voltage magnitudes in Table II require further scrutiny. The results in this section emphasize abundant caution in the use of remote as well as local non-traditional signals for feedback control designs in PSS units.

Table VII. SYSTEM ZEROS WHEN OUTPUTS ARE LINE ACTIVE POWER SIGNALS

Output signal			
P_{1-5}	P_{5-6}	P_{6-7}	P_{7-8}
0.0790+0.0000i	**0.0752+0.0000i**	**0.0990+0.0000i**	**0.0623+0.0000i**
-0.7961+1.4114i	**1.3026+0.0000i**	-0.4879+3.1158i	**3.1117+0.0000i**
-0.7961-1.4114i	-0.4876+4.9638i	-0.4879-3.1158i	-3.9824+0.6324i
-4.3219+0.0962i	-0.4876-4.9638i	-3.3707+0.1893i	-3.9824-0.6324i
-4.3219-0.0962i	-0.7870+7.4941i	-3.3707-0.1893i	-0.7791+7.4643i
-0.6177+5.0712i	-0.7870-7.4941i	-0.7898+7.4833i	-0.7791-7.4643i
-0.6177-5.0712i	-8.4346+0.2011i	-0.7898-7.4833i	-0.7766+8.1711i
-0.7872+7.4944i	-8.4346-0.2011i	-0.6420+8.0768i	-0.7766-8.1711i
-0.7872-7.4944i	-	-0.6420-8.0768i	-8.4316+0.1998i
-	-	-	-8.4316-0.1998i

P_{8-9}	P_{9-10}	P_{10-11}	P_{4-10}
-0.0005+0.0381i	-0.0002+0.0497i	**0.0738+0.0000i**	**0.0845+0.0000i**
-0.0005-0.0381i	-0.0002-0.0497i	-0.8118+7.9545i	-0.6505+6.6962i
3.1856+0.0000i	-0.7266+7.3788i	-0.8118-7.9545i	-0.6505-6.6962i
-4.0275+0.5929i	-0.7266-7.3788i	-1.2341+8.6904i	**7.1103+0.0000i**
-4.0275-0.5929i	-0.9875+8.1146i	-1.2341-8.6904i	-0.9232+8.0754i
-0.7789+7.4638i	-0.9875-8.1146i	**19.9993+0.0000i**	-0.9232-8.0754i
-0.7789-7.4638i	**10.7859+0.0000i**	**28.3275+22.9337i**	-9.0190+23.4422i
-0.7796+8.1725i	-1.8377+29.9188i	**28.3275-22.9337i**	-9.0190-23.4422i
-0.7796-8.1725i	-1.8377-29.9188i	-	-
-8.4456+0.2236i	-	-	-
-8.4456-0.2236i	-	-	-

B. SVC auxilary control design

SVCs are mainly used for dynamic voltage regulation of key buses in the power system. In this section, we study the design of supplementary small-signal stability control that introduces an additional stabilization loop in SVC by using a remote input signal. By employing remote signals, the inter-area oscillations can be mitigated as shown in many papers (e.g. [10]). In [20], it is analytically shown that depending on the system load level, the use of remote generator speed signals for SVC control can improve the damping of inter-area and or local modes in a simple power system.

In this section, an SVC with the capacity of ± 200MVAR , installed at Bus 8, is considered. Here the design of SVC auxiliary control is of interest, and the SVC voltage reference (i.e., V_{ref} of SVC) is set as the input. Note that the SVC voltage controller is not disabled and local bus voltage regulation is the primary control objective of the SVC. Three sets of outputs are considered; generator speeds, bus voltage magnitudes, and bus voltage angle difference signals for supplementary stability control.

1) Generator speed signals

Table VIII shows the system zeros when generator speed signals are selected as remote output signals. The zeros at origin are also observed in this case. It is interesting that except for generator 2, other generator speed signals do not show non-minimum phase behavior, and can be considered as potential choices for SVC damping control.

Table VIII . SYSTEM ZEROS WHEN OUTPUTS ARE GENERATOR SPEED SIGNALS

Output signal			
ω_1	ω_2	ω_3	ω_4
0.0000+0.0000i	0.0000+0.0000i	0.0000+0.0000i	0.0000+0.0000i
-2.2693+0.4115i	**0.1545+4.1356i**	-2.9257+0.3957i	-3.1247+0.2760i
-2.2693-0.4115i	**0.1545-4.1356i**	-2.9257-0.3957i	-3.1247-0.2760i
-0.0375+4.0367i	-0.0577+6.6158i	-0.4141+5.2752i	-0.6537+5.0079i
-0.0375-4.0367i	-0.0577-6.6158i	-0.4141-5.2752i	-0.6537-5.0079i
-0.7794+7.5147i	-0.7814+7.5152i	-0.7895+7.4504i	-0.0656+7.1225i
-0.7794-7.5147i	-0.7814-7.5152i	-0.7895-7.4504i	-0.0656-7.1225i
-1.5731+8.0532i	-	-1.7624+8.0436i	-0.7723+7.4363i
-1.5731-8.0532i	-	-1.7624-8.0436i	-0.7723-7.4363i
-8.8017+1.0061i	-	-9.7884+2.2522i	-
-8.8017-1.0061i	-	-9.7884-2.2522i	-

2) Bus voltage magnitude signals

Although the voltage magnitude signal of Bus 8 is already used as feedback signal in SVC voltage control loop, looking at bus voltage magnitude signals reveals a problem that might occur for calculation of infinite zeros.

Although (15) is the extended version of (7), sometimes, some of the calculated zeros by these equations are different. For example, let us consider a case when the output is considered as voltage magnitude of Bus 9 (see Table IX). Then, using (15), two zeros at $-1.2545*10^9$ and $1.2545*10^9$ are obtained, whereas using (7), two zeros at $35.90 + \text{i}\, 3.96*10^7$ and $35.90 - \text{i}\, 3.96*10^7$ are obtained. All other zeros are exactly same.

By investigating the transfer function relative degree, it is observed that the matrix multiplications $C_c B_c = 0$ and $C_c A_c B_c \neq 0$ hold. Thus, the transfer function relative degree is 2 [21]. It means that there are two infinite zeros. Further investigation shows that this is true when other bus voltage magnitude signals are considered as output signal. In other words, the two zeros calculated as large real or imaginary numbers are infinite zeros and due to numerical issues these are calculated as large finite values.

It can be seen from Table IX that except for the buses close to generators, other bus voltage magnitude signals (those which are close to SVC as well) have very small zeros, and the Bus 9 has no RHP zeros at all. As mentioned earlier, these small zeros are very sensitive to power flow solution and might be at LHP or at origin. Further investigation of the effect of equilibrium point accuracy should be performed for this case as well.

Table IX. SYSTEM ZEROS WHEN OUTPUTS ARE BUS VOLTAGE MAGNITUDE SIGNALS

Output signal			
V_1	V_2	V_3	V_4
0.0061+0.0000i	**0.0008+0.0029i**	**0.0054+0.0000i**	**0.0100+0.0000i**
1.5312+0.0000i	**0.0008-0.0029i**	-1.9674+0.4413i	**1.6208+0.0000i**
-1.7178+0.3297i	**0.7243+0.0000i**	-1.9674-0.4413i	-0.1951+4.4786i
-1.7178-0.3297i	-0.1787+4.5440i	**3.0291+0.0000i**	-0.1951-4.4786i
-0.1519+4.5177i	-0.1787-4.5440i	-0.2343+4.5199i	-0.6671+7.2737i
-0.1519-4.5177i	-0.6837+7.2404i	-0.2343-4.5199i	-0.6671-7.2737i
-0.6206+7.3003i	-0.6837-7.2404i	-0.6242+7.2964i	-0.7715+7.4918i
-0.6206-7.3003i	-0.7783+7.5115i	-0.6242-7.2964i	-0.7715-7.4918i
-7.3130+0.5429i	-0.7783-7.5115i	-7.3262+0.7709i	$4.9839*10^7$
-7.3130-0.5429i	$(0.0+4.9365i)*10^7$	-7.3262-0.7709i	$-4.9839*10^7$
-0.7793+7.5107i	$(0.0-4.9365i)*10^7$	-0.7621+7.4870i	-
-0.7793-7.5107i	-	-0.7621-7.4870i	-
$3.7437*10^7$	-	$(0.0+2.6407i)*10^7$	-
$-3.7437*10^7$	-	$(0.0-2.6407i)*10^7$	-

V_5	V_6	V_7	V_8
0.0322+0.0000i	**0.0045+0.0000i**	**0.0023+0.0000i**	**0.0002+0.0024i**
0.0872+0.0000i	-0.1981+4.5668i	-0.1961+4.5502i	**0.0002-0.0024i**
-1.9618+0.2319i	-0.1981-4.5668i	-0.1961-4.5502i	-0.1724+4.5117i
-1.9618-0.2319i	-0.6803+7.2695i	-0.7027+7.2861i	-0.1724-4.5117i
-0.1763+4.5876i	-0.6803-7.2695i	-0.7027-7.2861i	-0.7363+7.3006i
-0.1763-4.5876i	-0.7784+7.5108i	-0.7782+7.5106i	-0.7363-7.3006i
-0.6279+7.2451i	-0.7784-7.5108i	-0.7782-7.5106i	-0.7782+7.5104i
-0.6279-7.2451i	$(0.0+4.5940i)*10^7$	$7.4334*10^7$	-0.7782-7.5104i
-0.7789+7.5111i	$(0.0-4.5940i)*10^7$	$-7.4334*10^7$	$3.2375*10^{15}$
-0.7789-7.5111i	-	-	-
-8.1137+0.6596i	-	-	-
-8.1137-0.6596i	-	-	-
$4.9944*10^7$	-	-	-
$-4.9944*10^7$	-	-	-

V_9	V_{10}	V_{11}
-0.0002+0.0032i	**0.0452+0.0218i**	**0.0076+0.0000i**
-0.0002-0.0032i	**0.0452-0.0218i**	**1.2008+0.0000i**
-0.1644+4.4778i	-0.1628+4.4195i	-2.1421+0.2752i
-0.1644-4.4778i	-0.1628-4.4195i	-2.1421-0.2752i
-0.6972+7.2996i	-0.6696+7.2856i	-0.2239+4.3826i
-0.6972-7.2996i	-0.6696-7.2856i	-0.2239-4.3826i
-0.7687+7.5017i	-0.7682+7.4953i	-0.6287+7.2639i
-0.7687-7.5017i	-0.7682-7.4953i	-0.6287-7.2639i
-8.4335+0.0998i	$+9.2895*10^7$	-0.7674+7.4868i
-8.4335-0.0998i	$-9.2895*10^7$	-0.7674-7.4868i
$1.2545*10^9$	-	-8.2053+0.8321i
$-1.2545*10^9$	-	-8.2053-0.8321i
-	-	$(0.0+4.9938i)*10^7$
-	-	$(0.0-4.9938i)*10^7$

3) Bus voltage angle difference signals

System zeros when the output choice is bus voltage angle difference is presented in Table X. As can be seen from Table X, the problem of very small zeros appears in SVC case as well. In fact, angle difference signals which are across the system such as $\delta_6-\delta_{10}$ and $\delta_7-\delta_9$ show no non-minimum phase behavior, and can be considered as suitable candidates for SVC inter-area damping control signals.

Table X. SYSTEM ZEROS WHEN OUTPUTS ARE BUS VOLTAGE ANGLE DIFFERENCE SIGNALS

output signal			
$\delta_6-\delta_7$	$\delta_7-\delta_8$	$\delta_8-\delta_9$	$\delta_9-\delta_{10}$
0.0763+0.0000i	**0.0219+0.0000i**	**0.0002+0.0124i**	**0.0114+0.0000i**
1.6566+1.7819i	-4.2226+1.7100i	**0.0002-0.0124i**	-3.3482+4.5436i
1.6566-1.7819i	-4.2226-1.7100i	-2.4619+5.2970i	-3.3482-4.5436i
-2.4933+0.0735i	-0.6553+7.0296i	-2.4619-5.2970i	-0.7609+6.9463i
-2.4933-0.0735i	-0.6553-7.0296i	-0.8869+6.9515i	-0.7609-6.9463i
-0.6443+7.2152i	-0.7916+7.5341i	-0.8869-6.9515i	-0.7867+7.5372i
-0.6443-7.2152i	-0.7916-7.5341i	-0.7823+7.5376i	-0.7867-7.5372i
-0.7963+7.5229i	-7.6780+1.0180i	-0.7823-7.5376i	$2.2404*10^8$
-0.7963-7.5229i	-7.6780-1.0180i	-	-
-8.7449+0.1508i	-	-	-
-8.7449-0.1508i	-	-	-
$(-0.0-3.0288i)*10^8$	-	-	-
$(-0.0-3.0288i)*10^8$	-	-	-

$\delta_6-\delta_{10}$	$\delta_7-\delta_9$	$\delta_{10}-\delta_{11}$	$\delta_4-\delta_{10}$
0.0002+0.0110i	**0.0003+0.0082i**	**0.0134+0.0000i**	**0.0250+0.0000i**
0.0002-0.0110i	**0.0003-0.0082i**	-0.5649+5.7940i	-1.1930+4.7734i
-3.5206+4.8233i	-3.0331+5.1608i	-0.5649-5.7940i	-1.1930-4.7734i
-3.5206-4.8233i	-3.0331-5.1608i	-4.4238+5.2157i	-0.7735+7.4248i
-0.7662+6.9473i	-0.8172+6.9399i	-4.4238-5.2157i	-0.7735-7.4248i
-0.7662-6.9473i	-0.8172-6.9399i	-0.7862+7.4568i	**0.4709+7.6466i**
-0.7864+7.5371i	-0.7846+7.5374i	-0.7862-7.4568i	**0.4709-7.6466i**
-0.7864-7.5371i	-0.7846-7.5374i	$(-0.0+3.4376i)*10^8$	-8.4812+0.1474i
-	-	$(-0.0-3.4376i)*10^8$	-8.4812-0.1474i
-	-	-	$(-0.0+3.4003i)*10^8$
-	-	-	$(-0.0-3.4003i)*10^8$

IV. CONCLUSION

The paper studies the presence of non-minimum phase dynamics in the design of wide-area damping controllers. Two different case-studies are considered. In the first one, the zeros for PSS design based on both local and remote signals are examined. The second case studies the non-minimum phase zeros for SVC damping control design. For some input-output channels, numerical issues are observed. The effect of power-flow accuracy on the calculation of zeros which are very close to the origin requires further investigation. Moreover, it was shown that in some cases, infinite zeros appear as large finite RHP zeros which lead to misinterpretation of RHP zeros. For the SVC case, appropriate output signal candidates are suggested from the absence of RHP zeros.

REFERENCES

[1] D. Roberson and J. F. O'Brien, "Loop Shaping of a Wide-Area Damping Controller Using HVDC," in IEEE Transactions on Power Systems, vol. 32, no. 3, pp. 2354-2361, May 2017.

[2] J. Ma, Z. Y. Dong and P. Zhang, "Comparison of BR and QR Eigenvalue Algorithms for Power System Small Signal Stability Analysis," in IEEE Transactions on Power Systems, vol. 21, no. 4, pp. 1848-1855, Nov. 2006.

[3] Z. Du, W. Liu and W. Fang, "Calculation of rightmost eigenvalues in power systems using the Jacobi-Davidson method," in IEEE Transactions on Power Systems, vol. 21, no. 1, pp. 234-239, Feb. 2006.

[4] Schrader, Cheryl B., and Michael K. Sain. "Research on system zeros: a survey." International Journal of control 50, no. 4 (1989): 1407-1433.

[5] Hoagg, Jesse B., and Dennis S. Bernstein. "Nonminimum-phase zeros-much to do about nothing-classical control-revisited part II." IEEE control Systems 27, no. 3 (2007): 45-57.

[6] L. Zhang, H. P. Nee and L. Harnefors, "Analysis of Stability Limitations of a VSC-HVDC Link Using Power-Synchronization Control," in IEEE Transactions on Power Systems, vol. 26, no. 3, pp. 1326-1337, Aug. 2011.

[7] N. Martins, H. J. C. P. Pinto and L. T. G. Lima, "Efficient methods for finding transfer function zeros of power systems," in IEEE Transactions on Power Systems, vol. 7, no. 3, pp. 1350-1361, Aug 1992.

[8] N. Martins, P. C. Pellanda and J. Rommes, "Computation of Transfer Function Dominant Zeros With Applications to Oscillation Damping Control of Large Power Systems," in IEEE Transactions on Power Systems, vol. 22, no. 4, pp. 1657-1664, Nov. 2007.

[9] J. F. Hauer, "Robust damping controls for large power systems," in IEEE Control Systems Magazine, vol. 9, no. 1, pp. 12-18, Jan. 1989.

[10] M. M. Farsangi, Y. H. Song and K. Y. Lee, "Choice of FACTS device control inputs for damping interarea oscillations," in IEEE Transactions on Power Systems, vol. 19, no. 2, pp. 1135-1143, May 2004.

[11] M. M. Farsangi, H. Nezamabadi-pour, Y. H. Song and K. Y. Lee, "Placement of SVCs and Selection of Stabilizing Signals in Power Systems," in IEEE Transactions on Power Systems, vol. 22, no. 3, pp. 1061-1071, Aug. 2007.

[12] K. Koorehdavoudi et al., "Input-output characteristics of the power transmission network's swing dynamics," 2016 IEEE 55th Conference on Decision and Control (CDC), Las Vegas, NV, 2016, pp. 1846-1852.

[13] K. Koorehdavoudi et al., "Input-output properties of the swing dynamics for power transmission networks with HVDC modulation," to appear in Proceedings of the 20th IFAC World Congress, 2017.

[14] Small Signal Analysis Tool (SSAT), User's Manual, Powertech Labs Inc., Surrey, BC, Canada, 2002.

[15] P. Kundur, Power System Stability and Control, McGraw-Hill, 1994

[16] Misra, Pradeep, Paul Van Dooren, and Andras Varga. "Computation of structural invariants of generalized state-space systems." Automatica 30.12 (1994): 1921-1936

[17] E. V. Larsen and D. A. Swann, "Applying Power System Stabilizers Part I: General Concepts," in IEEE Transactions on Power Apparatus and Systems, vol. PAS-100, no. 6, pp. 3017-3024, June 1981.

[18] E. V. Larsen and D. A. Swann, "Applying Power System Stabilizers Part II: Performance Objectives and Tuning Concepts," in IEEE Transactions on Power Apparatus and Systems, vol. PAS-100, no. 6, pp. 3025-3033, June 1981.

[19] E. V. Larsen and D. A. Swann, "Applying Power System Stabilizers Part III: Practical Considerations," in IEEE Transactions on Power Apparatus and Systems, vol. PAS-100, no. 6, pp. 3034-3046, June 1981.

[20] N. Noroozian and G. Andersson, "Damping of inter-area and local modes by use of controllable components," in IEEE Transactions on Power Delivery, vol. 10, no. 4, pp. 2007-2012, Oct 1995.

[21] J. P. Corriou, Process Control: Theory and Applications, Springer, 2004.